NANO LETTERS

2008
Vol. 8, No. 1
302−306

Targeted Photothermal Lysis of the Pathogenic Bacteria, *Pseudomonas aeruginosa*, with Gold Nanorods

R. Sean Norman,[†] John W. Stone,[‡] Anand Gole,[‡] Catherine J. Murphy,[‡] and Tara L. Sabo-Attwood*,[†]

Department of Environmental Health Sciences, Arnold School of Public Health, Department of Chemistry and Biochemistry, University of South Carolina, Columbia, South Carolina 29208

Received October 19, 2007; Revised Manuscript Received November 21, 2007

ABSTRACT

Increases in the prevalence of antibiotic resistant bacteria require new approaches for the treatment of infectious bacterial pathogens. It is now clear that a nanotechnology-driven approach using nanoparticles to selectively target and destroy pathogenic bacteria can be successfully implemented. We have explored this approach by using gold nanorods that have been covalently linked to primary antibodies to selectively destroy the pathogenic Gram-negative bacterium, *Pseudomonas aeruginosa*. We find that, following nanorod attachment to the bacterial cell surface, exposure to near-infrared radiation results in a significant reduction in bacterial cell viability.

The global emergence of multidrug resistance (MDR) bacteria presents one of the greatest challenges facing public health care today.[1−3] For instance, it has been estimated that approximately sixty percent of nosocomial infections in the United States are caused by MDR bacteria.[4] Among the MDR bacteria, the Gram-negative bacterium, *Pseudomonas aeruginosa*, is a leading cause of infections and mortality among individuals with impaired immune function, such as patients with cystic fibrosis.[5−8] Given that *P. aeruginosa* and other pathogenic bacteria have evolved mechanisms of resistance for most commercially produced antibiotics, it is necessary to develop novel methods of antibacterial treatment that do not rely on traditional therapeutic regimes.

Recent advances in nanotechnology have provided the foundation for using metallic nanoparticles in the fight against MDR bacteria.[9−12] For instance, silver nanoparticles ranging from 1 to 10 nm in diameter have been shown not only to bind to the outer surface of bacteria but also to migrate intracellularly resulting in impaired cellular function and ultimately cell death.[11] However, the use of silver nanoparticles as therapeutic agents is potentially limited due to their nonspecific biological toxicity. More recently, gold nanoparticles have been used to target and destroy cancer cells, viruses, and bacteria.[10,12−19] Compared to silver, gold nanoparticles are more photostable, nontoxic, and amenable to surface modification based on the vast literature of self-assembled monolayers on flat gold surfaces.[20] Moreover, gold nanoparticles can be tuned to strongly absorb near-infrared (NIR) radiation depending on their shape,[21,22] and can ultimately transfer this energy into the surrounding environment as heat.[15,18,22] If the nanoparticles are attached to bacterial cells, the localized heating that occurs during NIR irradiation should cause irreparable cellular damage.

In this paper, we describe experiments in which gold nanorods are covalently conjugated with primary antibodies specific to the Gram-negative pathogen, *Pseudomonas aeruginosa*. The conjugated nanorods are then bound to *P. aeruginosa* cells, subsequently irradiated with NIR radiation, and the effect on cell viability monitored.

The *P. aeruginosa* isolate (PA3) used in this study was recently obtained from the upper respiratory tract of sinusitis patients. This isolate has a mucoid phenotype and demonstrates resistance to the antibiotics cipromycin, imipenem, and gentamicin. To generate primary antibodies for targeting nanorods to the PA3 cell surface, live bacteria were inoculated into rabbits followed by serum collection (Animal Pharm Services Inc., Healdsburg, CA). Polyclonal IgG antibody purification was performed using a commercially available Protein G agarose affinity column method following the manufacture's instructions (Invitrogen, Carlsbad, CA). Subsequent testing by immunblot analysis showed that the polyclonal antibody was highly specific against PA3 and did

* To whom correspondence should be addressed: Address: University of South Carolina, Department of Environmental Health Sciences, 921 Assembly St, PHRC 401, Columbia, South Carolina 29208. E-mail: saboattw@gwm.sc.edu.

[†] Department of Environmental Health Sciences, Arnold School of Public Health.

[‡] Department of Chemistry and Biochemistry.

10.1021/nl0727056 CCC: $40.75
Published on Web 12/07/2007

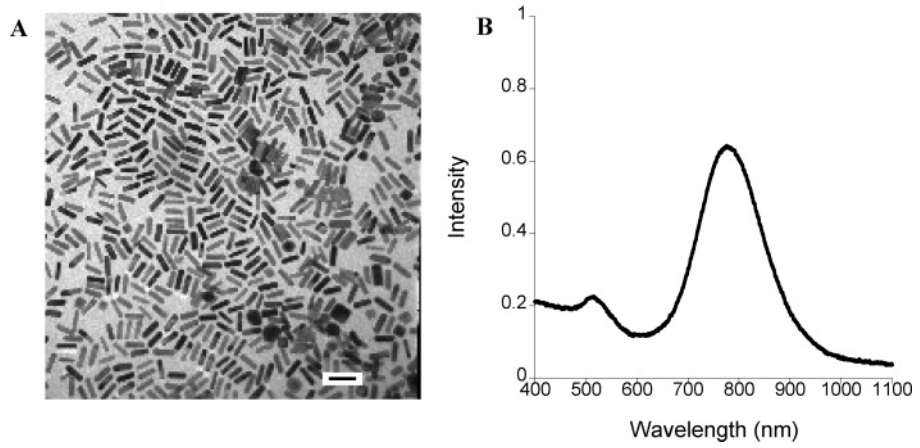

Figure 1. (A) TEM of 68 nm × 18 nm gold nanorods. Scale bar equals 100 nm. (B) UV−vis spectrum of the purified gold nanorods presenting an absorbance peak around 785 nm.

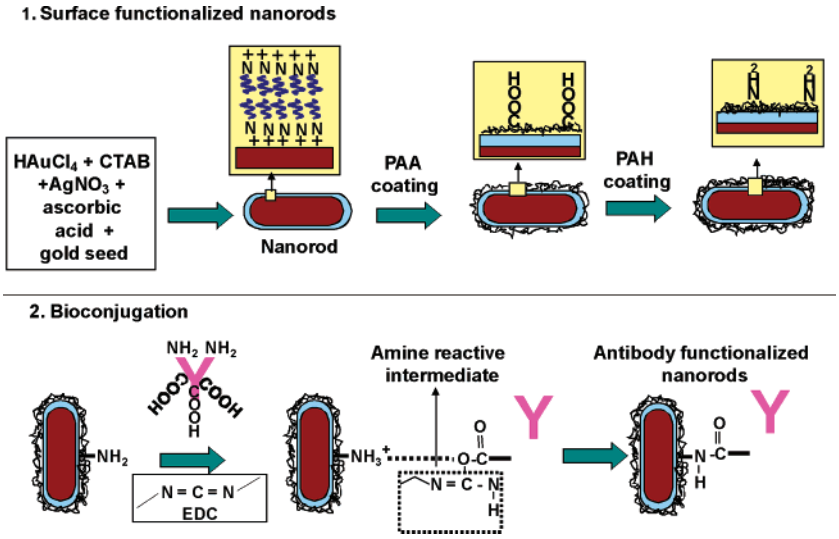

Figure 2. Scheme showing stages involved in the synthesis of IgG-conjugated gold nanorods.

not cross react with nonspecific targets (i.e., human lung cells; Supporting Information, Figure S1).

Gold nanorods with an aspect ratio ~4 were prepared in aqueous solution using a seed-mediated surfactant-directed approach and purified by centrifugation and washing as previously described.[21,23,24] The nanorods had a cationic surfactant, cetyltrimethylammonium bromide (CTAB) bound to their surfaces in the form of a bilayer.[25,26] The CTAB rendered the nanorods water stable and gave them a net positive charge. Figure 1A shows a representative transmission electron microscopy (TEM) of the gold nanorods used throughout this study. The 68 nm × 18 nm gold nanorods absorbed maximally at ~785 nm (Figure 1B). The addition of nanorods alone to PA3 bacterial cultures did not inhibit cell growth of the cultures over a 24 h period, suggesting that the nanorods were not inherently toxic to the cells (Supporting Information, Figure S2).

To target nanorods to PA3 cells, anti-PA3 primary antibodies were either electrostatically or covalently linked to the surface of the gold nanorods. Electrostatic linkage involved the direct addition of IgG to as-prepared rods containing CTAB without the use of 1-ethyl-3-(3-dimethylaminopropyl)-carbodiimide (EDC) or anionic poly(acrylic acid) (PAA) and cationic polyallylamine hydrochloride (PAH) coating followed by stirring for 30 min and purification by centrifugation. For covalent attachment, we utilized carboiimide chemistry. Briefly, purified gold nanorods, initially coated with CTAB, were further coated with two layers of polymers (PAA/PAH) by the layer-by-layer technique providing accessible amine groups to the solvent.[23] These amine-terminated nanorods were allowed to react with the carboxylic acids of purified antibodies for 12−16 h in the presence of EDC, a water-soluble carbodiimide that promotes amide bond formation between the carboxylic acid and primary amine.[23] Figure 2 shows the details of the EDC coupling procedure. Following incubation, the nanorod−antibody complexes were purified by centrifugation and resuspended in water/buffer. The unbound antibody in the supernatant solution was studied by fluorescence spectroscopy (Supporting Information, Figure S3, curves 2 and 3). The amount of antibody bound to the nanorods was determined by fluorescence (of free antibody in the supernatant after purification of nanorod−antibody conjugates, compared to total antibody added; Supporting Information,

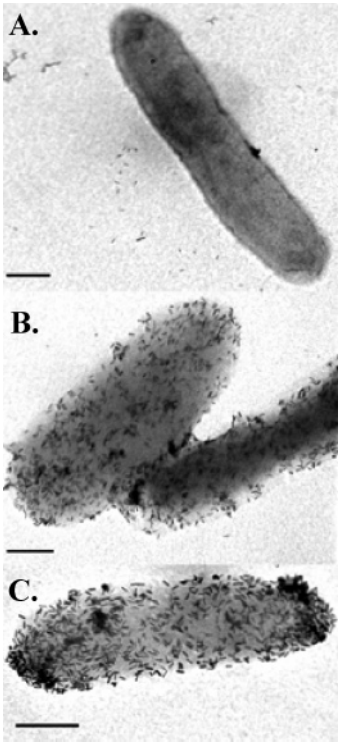

Figure 3. TEM images (30 000×) showing interaction of antibody conjugated nanorods with PA3. (A) PA3 with nonconjugated nanorods; (B) PA3 bound with electrostatically conjugated antibody−nanorod complexes; and (C) PA3 bound with covalently linked antibody−nanorod complexes using the EDC method. Scale bar equals 500 nm.

Figure S3, curve 4). On the basis of the calibration curve presented in the inset of Supporting Information, Figure S3, the relative concentrations of antibody bound to the rods for both covalent attachment and electrostatic coupling methods were calculated to be approximately 23.41 μg/mL.

The formation of nanorod-bound antibody complexes was determined by Fourier transform IR (FTIR) measurements (Supporting Information, Figure S4). The presence of amide I (∼1650 cm^{-1}) and III (1300−1200 cm^{-1}) bands in the electrostatically and covalently bound (curve 2 and 3, respectively) antibody−nanorod conjugates, which are comparable to the amide bands for free antibody, confirms the presence of antibody in the bioconjugate with intact secondary structures.[27]

Bacteria were allowed to incubate with the appropriate antibody−nanorod complexes for 20 min prior to prepping for TEM analysis as described in the Supporting Information. Images were collected on a Hitachi H-8000 TEM instrument operating at an accelerating voltage of 200 kV. TEM revealed that the bacteria were indeed covered with electron-dense gold nanorods (Figure 3). Although some bare nanorods bind to the bacterial cells (Figure 3A), the efficiency of binding was dramatically enhanced when the rods were attached to the PA3 specific antibodies, essentially covering the cell surface (Figure 3B,C). Antibody−nanorod complexes formed either by electrostatic or covalent conjugation methods were both found to efficiently target the bacteria. However, under physiological conditions (buffer and salt conditions), the covalently bound antibody−nanorod complex is more likely to be stable than its electrostatic counterpart. In the presence of salts, desorption of electrostatically bound antibody is highly probable, and hence for the rest of our studies, we focus mainly on using covalently attached antibody−nanorod complexes.

Following successful production of antibodies specific to *P. aeruginosa* and formation of functional EDC nanorod−antibody complexes, we performed experiments to determine if these targeted complexes could be used to destroy *P. aeruginosa* cells with NIR irradiation. Detailed methodology for the irradiation and fluorescent imaging of bacterial cells can be found in the Supporting Information. Briefly, PA3 cells were incubated for 20 min with antibody conjugated nanorods in 0.85% sodium chloride. The bacteria/nanorod mix was subsequently washed two times with 0.85% sodium chloride and resuspended in 5 μL 0.85% sodium chloride. The entire 5 μL bacteria/nanorod suspension was then exposed to NIR light (785 nm; ∼50 mW at the sample) for 10 min using a DeltaNu Advantage 785 Raman Laser System. This irradiation wavelength matched the longitudinal plasmon bands of the gold nanorods. Following irradiation, the bacteria were stained using a LIVE/DEAD kit (Invitrogen) following the manufacturer's instruction. The fluorescent microscopic images in Figure 4 show PA3 cells following treatments and after being stained with the LIVE (green)/DEAD (red) stains. Overall, exposing the targeted PA3 to NIR radiation resulted in a significant decrease in cell viability compared to unexposed bacteria. Quantification of these results is represented graphically as percent cell viability in the right panel. Counting of live versus dead cells showed that PA3 cells without nanorods or NIR (Figure 4A), NIR exposed cells without nanorods (Figure 4B), and cells with nanorods and no NIR exposure (Figure 4C) have approximately 80% cell viability, as seen by the predominance of "green" live cells. However, following exposure of nanorod-coated PA3 cells to NIR radiation (Figure 4D), there was a 75% decrease in cell viability corresponding to a significant ($P < 0.05$) increase in the number of dead or compromised cells, as indicated by the prevalence of "red" dead cells. These results reveal that the antibody-conjugated nanorods can be used to selectively target PA3 cells and, following NIR exposure, can be used to significantly reduce cell viability. To examine the extent of cellular membrane disruption following exposure of PA3 cells with attached nanorods to NIR radiation, cells were imaged by TEM. While the mechanism of nanorod-induced cell death is not clearly understood, the electron micrograph of the irradiated cells shows areas of massive irreparable cell membrane disruption, as indicated by the arrows in Figure 5. It has been suggested that cell membrane damage following nanoparticle exposure to NIR radiation could be due to numerous factors, including nanoparticle explosion, shock waves, bubble formation, and thermal disintegration.[10]

With the prevalence of MDR bacteria on the rise, it is necessary to explore alternative means of pathogen treatment. Our current study and others suggests that using nanoparticles to selectively target and destroy pathogenic microbial cells

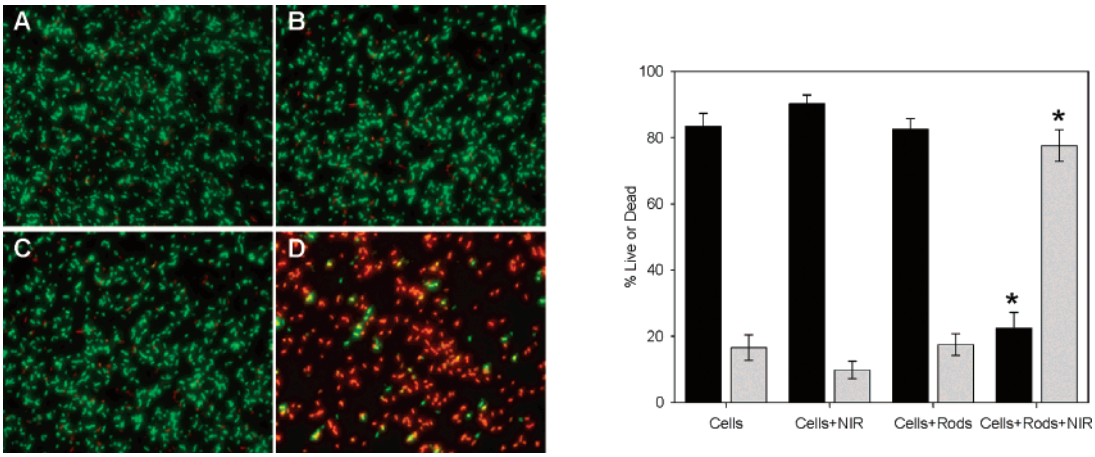

Figure 4. Viability of *Pseudomonas aeruginosa* cells with attached gold nanorods following exposure to NIR light. Left panels: (A) Control cells without nanorods or NIR exposure; (B) Cells without nanorods exposed to NIR; (C) Cells with nanorods and no NIR exposure; and (D) Cells with nanorods and exposed to NIR for 10 min. Cells were stained with SYTO 9 and propidium iodide and imaged at 400× magnification using a fluorescence microscope. Green fluorescent cells are representative of live cells while red fluorescent cells are representative of dead or compromised cells. The graph on the right shows the quantified LIVE/DEAD data. A total of 5 fields of view were counted per slide and each treatment was performed in triplicate. Black bars = percent live, Gray bars = percent dead. Significant differences from cells alone are marked with an asterisk (*) $P < 0.05$.

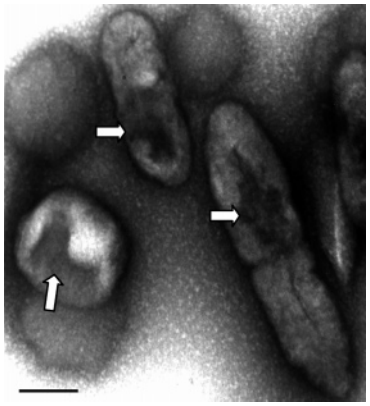

Figure 5. TEM image (30 000×) of PA3 cells with attached antibody-conjugated nanorods following 10 min exposure to NIR. The arrows indicate areas of the bacterial cell surface that have suffered irreparable damage. Scale bar equals 500 nm.

may be the next avenue for exploration. While others have shown that antibody-conjugated nanospheres can be used to kill bacteria following exposure to visible light,[12] our studies further enhance this technique by using nanorods that absorb in the NIR region, thus allowing deep penetration of radiation into tissues or highly resistant microbial biofilms. NIR radiation seems appropriate because researchers and clinicians are already using NIR light for optical imaging of tumors because the penetration depth can be up to 15 cm.[28−33] Furthermore, NIR is relatively harmless to tissues (at certain power levels), which make it an appropriate choice for localized heating of nanorods in vivo. Therefore, this method has promise for use in photothermalysis of persistent in vivo pathogenic bacterial biofilms or infections. Also, different from other studies that electrostatically attach secondary antibodies to nanospheres,[12] our approach utilizes primary antibodies covalently attached to the surface of nanorods. It is well known that under in vivo physiological conditions, that is, in the presence of salts, a reduction in electrostatic interactions would make electrostatically coupled nanorod−antibody complex less stable. As opposed to this, a covalently coupled antibody−nanorod complex is much more stable under these conditions. On the basis of the data presented here, it is clear that a nanotechnology-driven approach to treating antibiotic resistant bacteria is feasible and should continue to be developed and tested in in vivo model systems.

Acknowledgment. We would like to thank Dr. Lisa Steed from the Medical University of South Carolina's Diagnostic Microbiology Laboratory for providing us with the *Pseudomonas aeruginosa* PA3 isolate. We would also like to acknowledge Erin Beckman for technical assistance. This work was funded in part by the National Science Foundation (NSF CMMI 0555329).

Supporting Information Available: The experimental details of gold nanorod synthesis and IgG-nanorod conjugation are included along with corresponding fluorescent and FTIR spectra. Also, details regarding bacterial growth and irradiation are included. This material is available free of charge via the Internet at http://pubs.acs.org.

References

(1) Cosgrove, S. E.; Carmeli, Y. *Clin. Infect. Dis.* **2003**, *36*, 1433−1437.
(2) Cars, O.; Nordberg, P. *Antibiotic resistance—the faceless threat*, The Global Threat of Antibiotic Resistance: Exploring Roads towards Concerted Action; Uppsala, Sweden, 2004.
(3) Jones, R. N.; Pfaller, M. A. *Diagn. Microbiol. Infect. Dis.* **1998**, *31*, 379−388.
(4) Weinstein, R. A. *Emerging Infect. Dis.* **1998**, *4*, 416−420.
(5) Festini, F.; Buzzetti, R.; Bassi, C.; Braggion, C.; Salvatore, D.; Taccetti, G.; Mastella, G. *J. Hosp. Infect.* **2006**, *64*, 1−6.
(6) Gilligan, P. H. *Clin. Microbiol. Rev.* **1991**, *4*, 35−51.
(7) Hoiby, N.; Frederiksen, B.; Pressler, T. *J. Cystic Fibrosis* **2005**, *4* Suppl 2, 49−54.
(8) Lyczak, J. B.; Cannon, C. L.; Pier, G. B. *Microbes Infect.* **2000**, *2*, 1051−60.
(9) Hyland, R. M.; Beck, P.; Mulvey, G. L.; Kitov, P. I.; Armstrong, G. D. *Infect. Immun.* **2006**, *74*, 5419−5421.
(10) Letfullin, R. R.; Joenathan, C.; George, T. F.; Zharov, V. P. *Nanomedicine* **2006**, *1*, 473−480.

(11) Morones, J. R.; Elechiguerra, J. L.; Camacho, A.; Holt, K.; Kouri, J. B.; Ramirez, J. T.; Yacaman, M. J. *Nanotechnology* **2005**, *16*, 2346−2353.
(12) Zharov, V. P.; Mercer, K. E.; Galitovskaya, E. N.; Smeltzer, M. S. *Biophys. J.* **2006**, *90*, 619−27.
(13) El-Sayed, I. H.; Huang, X.; El-Sayed, M. A. *Nano Lett.* **2005**, *5*, 829−34.
(14) Chen, J.; Saeki, F.; Wiley, B. J.; Cang, H.; Cobb, M. J.; Li, Z.-Y.; Au, L.; Zhang, H.; Kimmey, M. B.; Li, X. D.; Xia, Y. *Nano Lett.* **2005**, *5*, 473−477.
(15) Chen, J.; Wang, D.; Xi, J.; Au, L.; Siekkinen, A.; Warsen, A.; Li, Z.-Y.; Zhang, H.; Xia, Y.; Li, X. D. *Nano Lett.* **2007**, *7*, 1318−1322.
(16) Chithrani, B. D.; Chan, W. C. W. *Nano Lett.* **2007**, *7*, 1542−1550.
(17) Chithrani, B. D.; Ghazani, A. A.; Chan, W. C. W. *Nano Lett.* **2006**, *6*, 662−668.
(18) Gobin, A. M.; Lee, M. H.; Halas, N. J.; James, W. D.; Drezek, R. A.; West, J. L. *Nano Lett.* **2007**, *7*, 1929−1934.
(19) Loo, C.; Lowery, A.; Halas, N.; West, J.; Drezek, R. *Nano Lett.* **2005**, *5*, 709−11.
(20) Love, J. C.; Estroff, L. A.; Kriebel, J. K.; Nuzzo, R. G.; Whitesides, G. M. *Chem. Rev.* **2005**, *105*, 1103−1170.
(21) Murphy, C. J.; Sau, T. K.; Gole, A. M.; Orendorff, C. J.; Gao, J.; Gou, L.; Hunyadi, S. E.; Li, T. *J. Phys. Chem. B* **2005**, *109*, 13857−70.
(22) El-Sayed, M. A. *Acc. Chem. Res.* **2001**, *34*, 257−64.
(23) Gole, A.; Murphy, C. J. *Langmuir* **2005**, *21*, 10756−62.
(24) Stone, J. W.; Sisco, P. N.; Goldsmith, E. C.; Baxter, S. C.; Murphy, C. J. *Nano Lett.* **2007**, *7*, 116−119.
(25) Nikoobakht, B.; El-Sayed, M. A. *Langmuir* **2001**, *17*, 6368−6374.
(26) Sau, T. K.; Murphy, C. J. *Langmuir* **2005**, *21*, 2923−9.
(27) Templeton, A. C.; Chen, S.; Gross, S. M.; Murray, R. W. *Langmuir* **1999**, *15*, 66−76.
(28) Brooksby, B.; Jiang, S.; Dehghani, H.; Pogue, B. W.; Paulsen, K. D.; Weaver, J.; Kogel, C.; Poplack, S. P. *J. Biomed. Opt.* **2005**, *10*, 051504.
(29) Houston, J. P.; Thompson, A. B.; Gurfinkel, M.; Sevick-Muraca, E. M. *Photochem. Photobiol.* **2003**, *77*, 420−30.
(30) Pogue, B. W.; Willscher, C.; McBride, T. O.; Osterberg, U. L.; Paulsen, K. D. *Med. Phys.* **2000**, *27*, 2693−700.
(31) Poplack, S. P.; Tosteson, T. D.; Wells, W. A.; Pogue, B. W.; Meaney, P. M.; Hartov, A.; Kogel, C. A.; Soho, S. K.; Gibson, J. J.; Paulsen, K. D. *Radiology* **2007**, *243*, 350−9.
(32) Srinivasan, S.; Pogue, B. W.; Brooksby, B.; Jiang, S.; Dehghani, H.; Kogel, C.; Wells, W. A.; Poplack, S. P.; Paulsen, K. D. *Technol. Cancer Res. Treat.* **2005**, *4*, 513−26.
(33) Srinivasan, S.; Pogue, B. W.; Jiang, S.; Dehghani, H.; Kogel, C.; Soho, S.; Gibson, J. J.; Tosteson, T. D.; Poplack, S. P.; Paulsen, K. D. *Acad. Radiol.* **2006**, *13*, 195−202.

NL0727056